environmental microbiology

Environmental Microbiology (2022) **24**(5), 2484–2501 doi:10.1111/1462-2920.15931

Cultivation and metabolic insights of an uncultured clade, Bacteroidetes VC2.1 Bac22 (*Candidatus* Sulfidibacteriales ord. nov.), from deep-sea hydrothermal vents

Hao Leng [1,2] **Weishu Zhao** [1,2] **and Xiang Xiao** [1,2,3*]

[1]*State Key Laboratory of Microbial Metabolism, School of Life Sciences and Biotechnology, Shanghai Jiao Tong University, Shanghai, China.*

[2]*International Center for Deep Life Investigation (IC-DLI), Shanghai Jiao Tong University, Shanghai, China.*

[3]*Southern Marine Science and Engineering Guangdong Laboratory (Zhuhai), Zhuhai, Guangdong, China.*

Summary

Bacteroidetes VC2.1 Bac22 (referred to as VC2.1) is an uncultured clade that is widely distributed in marine ecosystems, including hydrothermal vents, oxygen-minimum zones and other anoxic, sulfide-rich environments. However, the lack of cultured representatives and sequenced genomes of VC2.1 limit our understanding of its physiology, metabolism and ecological functions. Here, we obtained a stable co-culture of VC2.1 with autotrophic microbes by establishing an autotrophy-based enrichment from a hydrothermal vent chimney sample. We recovered a high-quality metagenome-assembled genome (MAG) that belonged to VC2.1. Phylogenetic analyses of both 16S rRNA genes and conserved protein markers suggested that VC2.1 belongs to a novel order in the Bacteroidetes phylum, which we named *Candidatus* Sulfidibacteriales. The metabolic reconstruction of this MAG indicated that VC2.1 could utilize polysaccharides, protein polymers and fatty acids as well as flexibly obtain energy via NO/N_2O reduction and polysulfide reduction. Our results reveal the ecological potential of this novel Bacteroidetes for complex organic carbons mineralization and N_2O sinks in deep-sea hydrothermal vents. Furthermore, guided by the genome information, we designed a new culture medium in which starch, ammonium and polysulfide were used as the carbon source, nitrogen source and electron acceptor respectively, to isolate VC2.1 successfully.

Received 9 June, 2021; revised 5 January, 2022; accepted 31 January, 2022. *For correspondence. E-mail zjxiao2018@sjtu.edu.cn; Tel: 0086-2134207206; Fax: 0086-2134204771;

Introduction

Bacteroidetes are the third most abundant bacterial group in the ocean, following by Proteobacteria and Cyanobacteria (Fernández-Gómez *et al*., 2013). This group is widespread in marine systems around the world, exhibits strong environmental adaptability and accounts for a large proportion of marine plankton (Kirchman, 2002; Pommier *et al*., 2007). In marine environments, Bacteroidetes are generally believed to prefer to attach to the surface of particles or algae cells and specialize in the degradation of compounds with high molecular weights (e.g. protein polymers, polysaccharides, etc.) by using a large number of genes related to peptidases, glycoside hydrolases (GHs) and glycosyltransferases (Suter *et al*., 2018; Unfried *et al*., 2018; Krüger *et al*., 2019). Therefore, they are an important contributor to the mineralization of complex organic substrates such as proteins and polysaccharides (Kabisch *et al*., 2014; Reintjes *et al*., 2017).

Compared to the number of studies on Bacteroidetes living in the human gut or surface marine environments, many fewer studies have investigated deep-sea Bacteroidetes groups, especially those living in oxygen-deficient zones. VC2.1 was first reported from a hydrothermal vent in the Mid-Atlantic Ridge (Reysenbach *et al*., 2000). It was named after the first clone found in this group, VC2.1 Bac22 (NCBI accession: AF068798), which was discovered during a diversity analysis of a chimney cap placed *in situ* for 5 days on a hydrothermal vent at which the temperature fell from 70°C to 20°C. Another study on the East Pacific Rise found that VC2.1 was dominant in inactive hydrothermal sulfide chimney samples, accounting for 17% of all clones, and was detected in six of seven samples (Sylvan *et al*., 2012). In a post-eruption 'snowblower' vent at Juan de Fuca Ridge, VC2.1 was more abundant in the white floc inside

the venting orifice than in the diffused fluid (Meyer *et al*., 2013), which indicates their preference for a particle-associated lifestyle. The phylogenetic analysis of the 16S rRNA genes in these clone libraries showed that these Bacteroidetes formed an independent clade in the Bacteroidetes phylum. Sequences of this clade were found only in samples from sulfide-rich environments, so it was named 'Sulfiphilic Bacteroidetes', and it was assumed that this clade requires reduced sulfur for its growth (Sylvan *et al*., 2013). To date, in the Silva database, VC2.1 is still an uncultured order in the Bacteroidetes phylum; VC2.1 is detected mainly in inactive sulfide environments or sulfide-rich environments (e.g. active hydrothermal vents, oxygen-minimum zones, sediments) (Reysenbach *et al*., 2000; Sievert *et al*., 2000; Alain *et al*., 2002; Teske *et al*., 2002; Dhillon *et al*., 2003; Alain *et al*., 2004; Walsh *et al*., 2009; Lanzén *et al*., 2011; Sylvan *et al*., 2012; Wright *et al*., 2012; Meyer *et al*., 2013; Sylvan *et al*., 2013; Kato *et al*., 2015; Steinle *et al*., 2018). Despite extensive observations of VC2.1, cultivations and related genomic information have not yet been successfully obtained, limiting our understanding of the metabolic characteristics and ecological functions of VC2.1.

In this study, we incorporated environmentally simulated cultivation and non-cultivated metagenomics analysis to analyse samples from deep-sea hydrothermal vents. Then, we classified VC2.1 as a new order in the Bacteroidetes phylum. Metabolic reconstruction based on the MAG of VC2.1 revealed its variable and flexible metabolic capabilities with regard to both substrate utilization (e.g. polysaccharides, proteins, fatty acids) and energy processes (e.g. sulfur reduction, nitric oxide, nitrous oxide reduction). Furthermore, guided by the metagenomic analysis, we successfully isolated VC2.1, and experimentally measured its physiological utilization of various carbon sources and electron acceptors. In this work, we obtained a stable co-culture and an isolate of VC2.1, and shed light on the ecological potentials of VC2.1 for carbon, nitrogen and sulfur cycling in deep-sea hydrothermal vents.

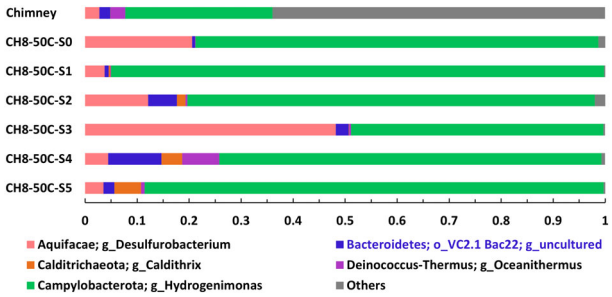

Fig. 1. Microbial community composition of the chemoautotrophic enrichment community at the genus level. Coloured bars indicate the percentage of the designated group within each sample. Only those classes with *Desulfurobacterium*, Bacteroidetes; o_VC2.1 Bac22; g_uncultured, *Calditrix*, *Oceanithermus* and *Hydrogenimonas* are listed. The remaining sequences are combined in the 'Others' category. Labels: Chimney, the chimney sample; CH8-50C-S0, original chemoautotrophic enrichment; CH8-50C-S1 (to CH8-50C-S5), the first (to fifth) subcultures transferred from the original chemoautotrophic enrichment.

Results

Establish a stable Bacteroidetes-containing community

The original sample was collected on the East Pacific Rise from an active black smoker chimney emitting hydrothermal fluid at a temperature of 231°C. A chemoautotrophic enrichment environment was initially established to simulate the natural environment according to the chemoautotrophy-based features of the hydrothermal vent ecosystem (Sievert and Vetriani, 2012). We successfully performed the original enrichment at 50°C. Then, a five-round transfer was carried out in the same chemoautotrophic medium under strictly anaerobic conditions until the maximum cell number reached $\sim 1 \times 10^8$ cells ml^{-1}. We monitored and ensured the stability of the microbial community composition by amplicon sequencing (Fig. 1). The results suggested that autotrophic Campylobacterota (formerly Epsilonproteobacteria) (Waite *et al*., 2017) and Aquificae and heterotrophic Calditrichaeota, Deinococcus-Thermus and Bacteroidetes were the main taxa co-clustered in the enriched culture. In the original chimney sample, the above autotrophic groups accounted for 31%, and the above heterotrophic groups accounted for 5% of the bacterial community. After enrichment under chemoautotrophic conditions, the relative abundance of autotrophic microbes increased to 78.0%–98.6%, especially that of *Hydrogenimonas* in Campylobacterota (up to 94.8%). The heterotrophic bacteria made up 0.6%–21.3% of the total community, of which uncultured VC2.1 accounted for 0.5%–10.3%.

Recovery of population genomes from the metagenomic dataset

To uncover the metabolic characteristics of VC2.1 and the metabolic interactions of the chemoautotrophic community, the enriched culture was subjected to metagenomic sequencing after the fifth round of enrichment. After sequencing quality controls, 158 301 658 paired reads ($\sim$44 Gb of 2 $\times$ 150 bp Illumina reads) were assembled and binned (see Experimental procedures). Six MAGs were obtained from the metagenomic dataset (Table 1). All six MAGs had completeness ranging from 84.92% to 99.58%, and contamination ranging from 0.54% to 2.44%. The size of six MAGs ranged from 1.2

Table 1. Statistical summary of the chemoautotrophic enrichment genomes.

Bin ID	Bin1	Bin2	Bin3	Bin4	Bin5	Bin6
Completeness (%)[a]	99.58	98.97	84.92	96.77	97.74	91.49
Contamination (%)[a]	1.22	2.44	1.27	0.54	1.1	2.13
Strain heterogeneity (%)[a]	0	0	33.33	0	0	0
Genome size (bp)	2 337 999	2 215 757	1 271 657	3 185 313	3 452 875	2 063 629
Relative abundance (%)	75.82	7.16	0.05	1.40	8.16	4.27
GC (%)	58.94	55.16	39.61	42.42	46.75	63.43
Scaffolds	9	20	137	53	300	44
Longest scaffold (bp)	847 476	375 431	46 100	331 799	97 907	194 083
N50 (scaffolds) (bp)	637 680	165 018	17 513	107 512	17 770	71 768
Predicted genes	2295	2186	1421	2578	2817	2014
Coding density (%)	93.84	93.33	94.72	89.58	89.35	91.88
5S rRNA genes	1	–	1	1	–	1
16S rRNA genes	1	–	1	1	–	1
23S rRNA genes	1	–	1	1	–	–
tRNA genes	45	44	41	46	36	43
Taxonomy	*Hydrogenimonas*	*Hydrogenimonas*	*Desulfurobacterium*	Bacteroidetes VC2.1 Bac22	*Caldithrix*	*Oceanithermus*
predOGT (°C)[b]	52.41	51.23	65.34	38.37	53.89	50.43

[a]Genome completeness, contamination and strain heterogeneity were determined by CheckM.
[b]Optimal growth temperature predicted by machine learning software (Tome).

to 3.3 Mb, and the GC content ranged from 39.61% to 63.43% (Table 1). By mapping the clean reads to the binned genomes, the sum of sequences in these six MAGs covered 96.86% of the total metagenomic reads, which indicated that these six MAGs represented the enriched community well. The relative abundance of the autotrophic groups (Bin 1, Bin 2, Bin 3) was 83.03%, and Bin 1 accounted for up to 75.82% of the total reads. However, heterotrophic microbes (Bin 4, Bin 5, Bin 6) accounted for 13.83% of the total reads. The ratio of autotrophy to heterotrophy (83.03%/13.83%) is compatible with the ratio estimated by the amplicon sequencing described above (91.74%/7.94%). Among six MAGs, three (i.e. Bin1, Bin4, Bin6) matched the high-quality standard according to Minimum Information about a Metagenome-Assembled Genome (Bowers *et al*., 2017). Among them, the 16S rRNA gene of Bin 4 indicated that it belonged to VC2.1. The size of Bin 4 was 3 185 313 bp, with 96.77% completeness and 0.54% contamination.

Phylogenetic classification of VC2.1

The phylogenetic affiliations of the enriched genomes were examined first by analysing the full-length 16S rRNA gene sequences in the bins. The phylogenetic analysis of the 16S rRNA genes revealed that Bin 4 was distinct from all known Bacteroidetes orders containing cultured representatives (Fig. 2A) but was affiliated with the uncultured order-level lineage VC2.1 (Fig. 2B). The phylogeny showed that some VC2.1 sequences in the Silva 132 database belonged to a novel, order-level lineage. We temporarily named this novel order-level clade after Bacteroidetes GBS-CoSAG_01, which is the first reported genome in this order (Doud *et al*., 2019). All known sequences in this clade were obtained from terrestrial environments (Fig. S1). However, the sequences in VC2.1 were obtained mostly from marine environments (Fig. 2B). Comparing the sequence similarity by BLASTn, the closest cultured representative to Bin 4 was *Wandonia haliotis* NBRC 105642, with 88.58% nucleotide identity (Table S1). This identity is lower than the median sequence identity for novel orders (Yarza *et al*., 2014), suggesting that Bin 4 represents a novel order. Bin 4 was also close to the first reported clone in this order, VC2.1 Bac22 (OTU12 in Fig. 2B, 95.45% identity) (Reysenbach *et al*., 2000). The sequence similarity of the 16S rRNA gene sequences in VC2.1 ranged from 83% to 97% (Table S2), indicating the high diversity in this group.

An analysis based on 43 universally conserved protein sequences further supported that Bin 4 formed a robustly monophyletic group that was distinct from all cultured Bacteroidetes orders (Fig. 3). The average amino acid identity (AAI) of Bin 4 against representative genomes of cultured Bacteroidetes orders ranged from 48.55% to 56.27% (Table S3), which also suggested that Bin 4 represents a novel order (Konstantinidis and Tiedje, 2005a; Hugenholtz *et al*., 2016). Overall, the phylogenetic analyses of both the 16S rRNA gene and the 43 concatenated markers confirmed Bin 4 as a novel order in the Bacteroidetes phylum. Herein, we propose the name '*Candidatus* Sulfidibacterium hydrothermale'

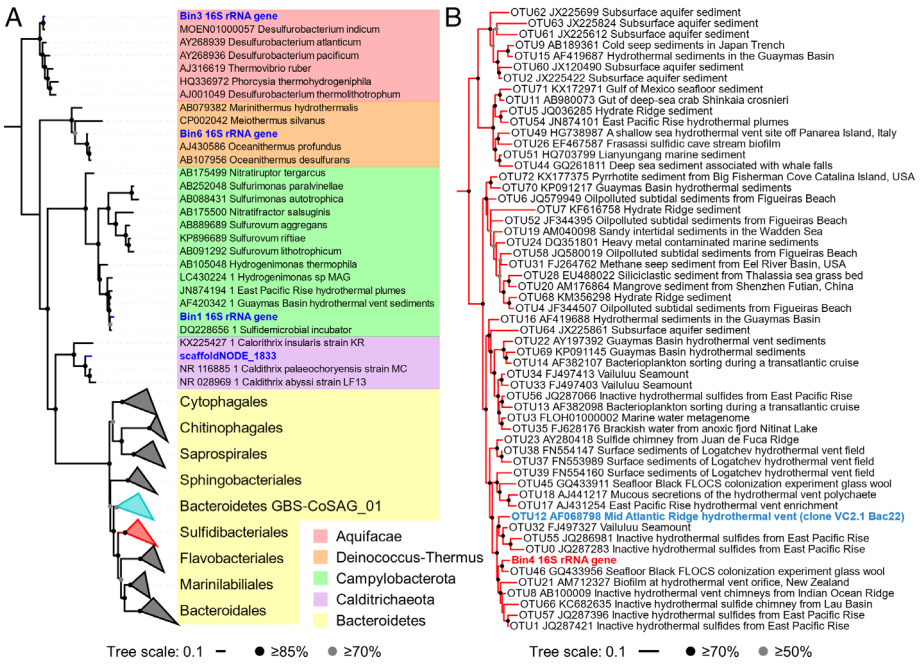

Fig. 2. Maximum-likelihood phylogeny of the 16S rRNA genes.
A. Phylogeny of the enriched chemoautotrophic community. The reference sequences of Bacteroidetes VC2.1 Bac22 (*Ca*. Sulfidibacteriales) were downloaded from the Silva database (Silva 132), sequences smaller than 1400 bp were filtered out, and OTUs were identified from the remaining sequences with a cut-off of 97%. The phylogeny showed that some VC2.1 sequences in the Silva 132 database belonged to a novel order-level lineage, and we temporarily named this lineage Bacteroidetes GBS-CoSAG_01.
B. Phylogeny of Bacteroidetes VC2.1 Bac22. The tree was inferred with IQ-TREE with the '-MFP' options for best-fit model selection and 1000 ultrafast bootstrap replicates. The scale bar represents 0.1 nucleotide substitutions per sequence position.

gen. nov., sp. nov. for Bin 4, referring to its occurrence in sulfidic habitats, and its geographical origin from a hydrothermal vent on the East Pacific Rise, and the name '*Candidatus* Sulfidibacteriales' ord. nov. for the lineage previously known as Bacteroidetes VC2.1 Bac22.

Metabolic capabilities of Ca*. S. hydrothermale*

Carbon metabolism. Bacteroidetes are well known for their metabolic diversity with the ability to degrade carbohydrates and other complex organic compounds through respiration or fermentation. A similar diverse capability was observed in the genome of *Ca*. S. hydrothermale. Genes involved in glycolysis, the gluconeogenesis pathway, the TCA cycle and the pentose phosphate pathway were all identified (Fig. 4), as well as numerous genes involved in other sugar metabolism, including mannose metabolism (mannose-1-phosphate guanylyltransferase, mannose-6-phosphate isomerase, phosphomannomutase), fructose metabolism (fructokinase), cellulose degradation (beta-glucosidase) and starch metabolism (alpha-amylase, TonB-dependent starch-binding outer membrane protein (*susC*), starch-binding outer membrane protein (*susD*) (Tables S4, S5). In addition, genes involved in fatty acid degradation (acyl-CoA dehydrogenase, 3-hydroxybutyryl-CoA dehydrogenase, acetyl-CoA acyltransferase) were identified in the genome of *Ca*. S. hydrothermale (Table S4). Furthermore, peptidase-related genes (Table S6) were also detected in the genome, indicating the potential for protein hydrolysis by *Ca*. S. hydrothermale. In addition, genes identified as being involved in acetate metabolism (phosphate acetyltransferase, acetate kinase, acetyl-CoA synthetase, acetate-CoA ligase) revealed that *Ca*. S. hydrothermale may gain ATP by producing acetate.

Nitrogen and sulfur metabolism. The genome of *Ca*. S. hydrothermale revealed the possibility of utilizing various electron acceptors, especially nitrogen and sulfur compounds, to gain energy. The results also suggested the potential function of *Ca*. S. hydrothermale is related to N and S cycling *in situ*. *Ca*. S. hydrothermale contains *norB* and *nosZ* genes, which are involved in the denitrification pathway. The gene encodes nitric oxide reductase (Nor), which is an iron-containing enzyme that catalyses the reduction of nitric oxide (NO) to nitrous oxide (N_2O) (Hino *et al*., 2010). Nitrous oxide reductases (Nos) catalyse the two-electron reduction of N_2O to N_2 (Brown *et al*., 2000). Moreover, an ammonium transporter gene (*amt*) was also detected in the genome, which suggests that *Ca*. S. hydrothermale may assimilate ammonium as a nitrogen source for biosynthesis. Genes for assimilatory sulfate reduction (*cysNC*, *cysD*, *cysC*, *cysH*) were also identified in *Ca*. S. hydrothermale. Other sulfur-related genes identified in the genome included polysulfide reductase chain A (*psrA*) and sulfide:quinone oxidoreductase (*sqr*). Polysulfide reductase could be a key energy-conserving enzyme in the respiratory chain, using polysulfide as the terminal electron acceptor and pumping protons across the membrane (Jormakka *et al*., 2008). Sulfide:quinone oxidoreductase is a flavoprotein with homologues in all domains of life except

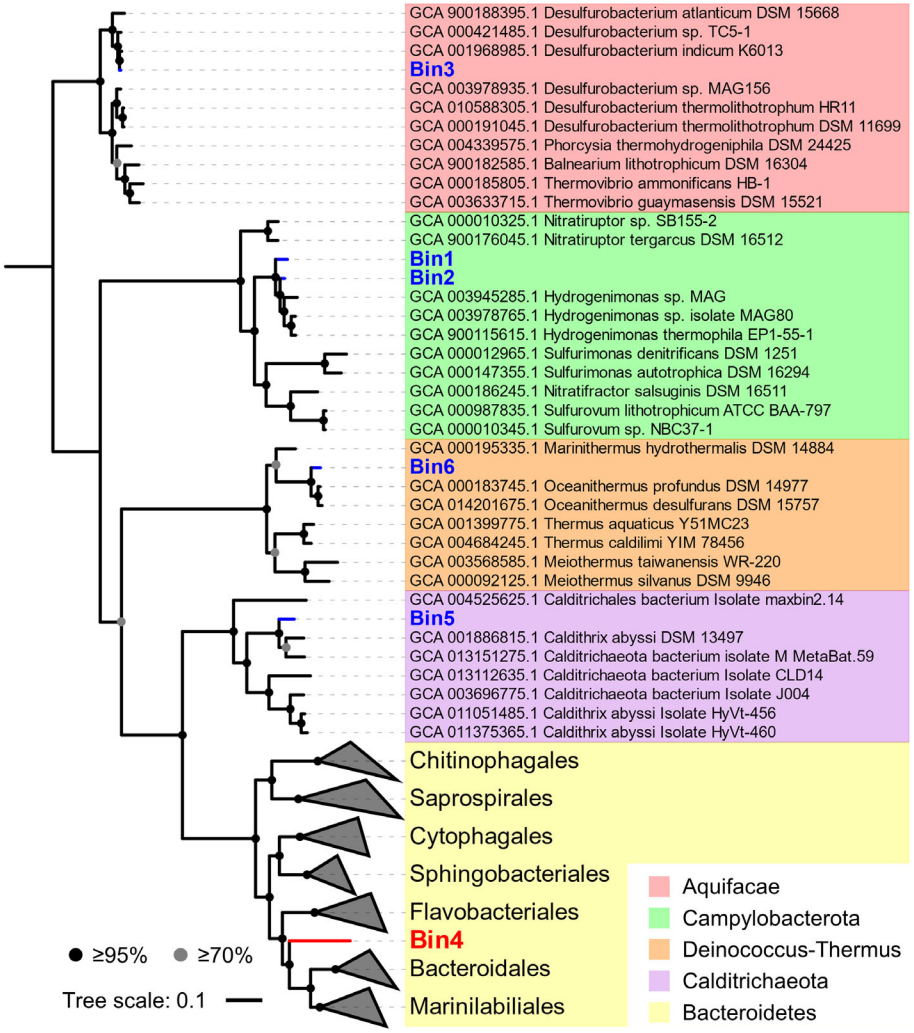

Fig. 3. Phylogenomic tree of Bacteroidetes VC2.1 Bac22 and other chemoautotrophic enrichment bacteria. A phylogenomic tree of 43 concatenated conserved proteins was inferred with IQ-TREE with the '-MFP' option for best-fit model selection and 1000 ultrafast bootstrap replicates. Bootstrap support values ≥95% are shown as black circles on nodes; bootstrap support values ≥70% are shown as grey circles on nodes. The scale bar represents 0.1 amino acid substitutions per sequence position.

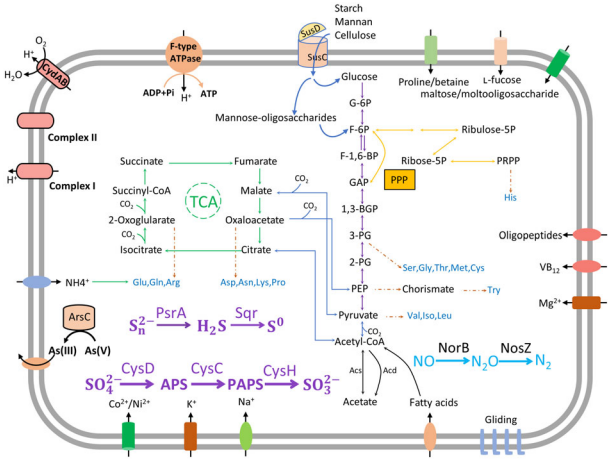

Fig. 4. Schematic diagram of the key metabolic pathways in *Ca*. S. hydrothermale. *Ca*. S. hydrothermale exhibits complete glycolysis, the TCA cycle, and the PP pathway and can utilize organic substances such as glycans, maltose, fructose, oligopeptides and fatty acids. The list of the annotated genes is provided in Table S4.

plants that play a physiological role in both sulfide detoxification and energy transduction (Marcia *et al*., 2009).

Oxygen and arsenic metabolism. Although the experimental conditions were anaerobic, oxygen-respiration related genes of cytochrome bd oxidase (*cydA*, *cydB*) were still detected. Cytochrome bd oxidase is a respiratory oxidase found only in prokaryotes. The enzyme is reportedly characterized by a high affinity for O_2; accordingly, it is preferentially expressed under low-O_2 stress (Giuffrè *et al*., 2014), which indicates the capacity for *Ca*. S. hydrothermale to grow microaerobically. This capacity allows this type of bacteria to live in habitats where the reduced hydrothermal fluid and the oxidized seawater are irregularly and nonuniformly mixed. Elevated concentrations of potentially toxic heavy metals, such as arsenic, are present in hydrothermal vents, leading to the development of heavy metal resistance in the resident

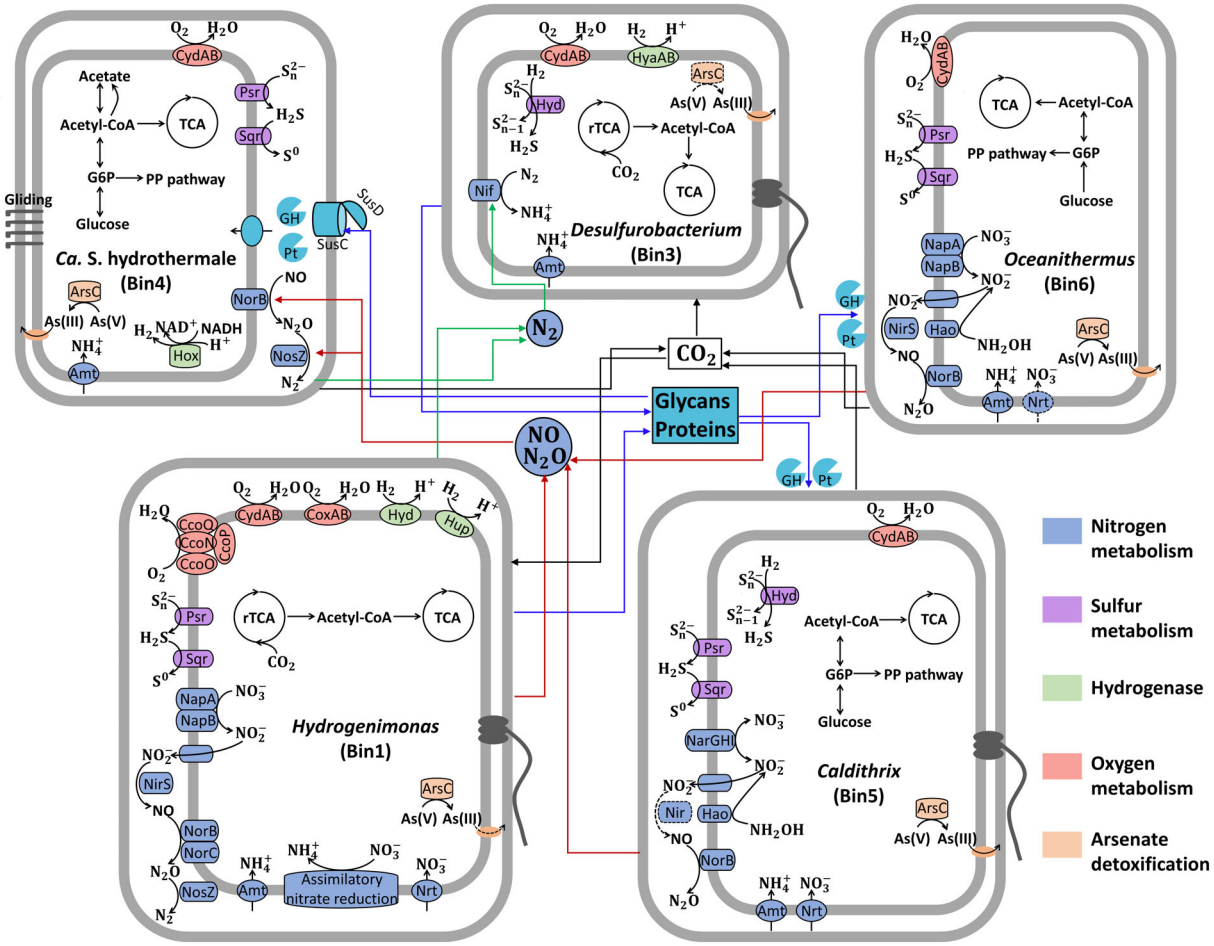

Fig. 5. Schematic diagram of the microbial metabolic network in the chemoautotrophic enrichment community. A dotted line indicates that a gene was not identified. GH, glycoside hydrolase; Pt, peptidase; TCA, tricarboxylic acid cycle; rTCA, reverse tricarboxylic acid cycle; PP pathway, pentose phosphate pathway. The other gene names are provided in Table S7. Blue arrows indicate the exchange of glycans and proteins. Black arrows indicate the exchange of CO_2. Red arrows indicate the exchange of N_2O and NO. Green arrows indicate the exchange of N_2.

microbiota (Patwardhan *et al*., 2020). Genes involved in the detoxification of arsenate (*arsC*) were identified in the *Ca*. S. hydrothermale genome. Arsenate detoxification is catalysed by reductases (ArsC), with homology to the glutaredoxin family (ArsC1), to low-molecular-weight phosphatases (ArsC2) (Chen *et al*., 2020). The genome of *Ca*. S. hydrothermale contains both ArsC1 and ArsC2 as well as the arsenite-transporting ATPase (ArsA), suggesting its capacity to reduce arsenic to arsenite and then transport arsenite out of the cell with the ArsA transporter.

Metabolic interactions in the enriched microecosystem

We further constructed the metabolic network of the enriched microecosystem to investigate the potential metabolic interactions between autotrophic and heterotrophic microorganisms based on metagenome analysis (Fig. 5). The autotrophs in the enriched microecosystem were *Hydrogenomonas* and *Desulfurobacterium*, which belong to ecologically significant autotrophic groups Campylobacterota and Aquificae respectively, in hydrothermal vents (Nakagawa and Takai, 2008). *Hydrogenomonas* isolations were reported to be chemolithoautotrophs capable of using molecular hydrogen as the sole energy source and molecular oxygen, nitrate or sulfur species ($S_2O_3^{2-}$, S^0) as electron acceptors to support growth (Mino *et al*., 2021). Our enriched *Hydrogenomonas* shows the same capability in the genome for both carbon fixation and electron donors/acceptors. *Desulfurobacterium* strains were reported to be able to oxidize hydrogen with the reduction of nitrate or sulfur species ($S_2O_3^{2-}$, SO_3^{2-}, S^0) (Cao *et al*., 2017). However, the enriched *Desulfurobacterium* in this study was annotated only to be a sulfur reducer. For the heterotrophs in the enriched microecosystem, *Caldithrix* and *Oceanithermus* were the other two groups besides Bacteroidetes mentioned above (Mori *et al*., 2004;

Miroshnichenko *et al*., 2010). Both *Caldithrix* and *Oceanithermus* show the potential to utilize both sulfur and nitrate as electron acceptors to degrade proteins and glycans (Fig. 5).

In the enriched microecosystem, for carbon cycling, extracellular polysaccharides, proteins and other organic matter secreted by autotrophic microorganisms, along with the cell contents released after the death of bacteria, can be utilized by co-cultured heterotrophic microorganisms. Carbon dioxide produced by heterotrophic microorganisms during the degradation of this organic matter can be used as a carbon source for autotrophy. Nitrogen and sulfur cycling seems to be the main drivers of energetic processes in the enriched ecosystem. The presence of sufficient nitrate in the enrichment medium resulted in an abundance of genes related to nitrogen metabolism in the enriched community. *Ca*. S. hydrothermale can reduce the accumulation of intermediates (nitric oxide and nitrous oxide) produced by the co-cultured microbes (i.e. *Hydrogenomonas*, *Caldithrix* and *Oceanithermus*) during incomplete denitrification by converting these compounds to N_2. And N_2 can be further immobilized by *Desulfurobacterium* to generate ammonia to complete the nitrogen cycle (Fig. 5; Table S7). For sulfur cycling, all microbes in the enriched microecosystem can reduce polysulfide to H_2S via various enzymes: polysulfide reductase chain A (PsrA), sulfhydrogenase (Hyd) (Ma *et al*., 1993; Jormakka *et al*., 2008) (Fig. 5; Table S7). Besides the polysulfide respiration, polysulfide can also be used as an electron donor. In the genome of *Hydrogenomonas*, the predominant primary producer in the co-culture, genes of both sulfide oxidation (Sqr), nitrate and oxygen reduction have been identified (Fig. 5), which indicated a potential coupling of the sulfide oxidation with nitrate or/and oxygen reduction. This Sqr-involved sulfide oxidation with nitrate was also proposed in a chemolithotrophic Deltaproteobacterium *Desulfurivibrio alkaliphilus* (Thorup *et al*., 2017). In conclusion, the metabolic complementarity of these microbes allowed substrates to be fully recycled in the enriched community; *Ca*. S. hydrothermale potentially plays an essential role in both the C, N and S cycles in the microecosystem.

Metagenome-guided isolation of Ca*. S. hydrothermale*

Starting from the stable co-culture of VC2.1 with autotrophs, we further modified the carbon and nitrogen sources in the medium and cultivation temperature to isolate *Ca*. S. hydrothermale based on information from metagenomic analysis (Fig. 6A). The genome annotation of *Ca*. S. hydrothermale revealed its capability to utilize polysaccharides (starch, mannan, etc.) as the carbon source and polysulfide as the electron acceptor. The incomplete denitrification pathway of *Ca*. S. hydrothermale suggested that nitrate is not an electron acceptor for the growth of *Ca*. S. hydrothermale. However, the presence of the ammonium transporter gene suggested ammonium as a possible nitrogen source. Furthermore, a machine learning model predicted that the optimal growth temperature for *Ca*. S. hydrothermale was 38°C based on its genome (see Experimental procedures) (Table 1). According to the above information, we designed a new modification for SME medium (see Experimental procedures) that involved removing nitrate and adding starch as the sole carbon source, polysulfide as the electron acceptor and ammonium as the nitrogen source. This medium was solidified with 1.5% (wt./vol.) agar in anaerobic rolling tubes. Then, the chemoautotrophic community enriched at 37°C was transferred to the prepared rolling tubes and incubated at 37°C. Seven days later, single colonies had grown on the solid medium; they were 1.0–2.0 mm in diameter, circular, flat and white (Fig. S2). We randomly picked five colonies from around 10 total colonies, to identify the 16S rRNA with the primer B27F/U1492R (DeLong, 1992). The 16S rRNA gene sequencing results of all these five colonies were the same as the 16S rRNA in MAG Bin4 (aligned length 1347 bp), which is in the same clade as the representative clone VC2.1 Bac22 (OTU12) based on the phylogenetic tree (Fig. 2B). After obtaining a single colony, the purity of the culture was determined through both the 16S rRNA gene sequencing results and morphological observation by electron microscopy. *Ca*. S. hydrothermale were observed to be rod-shaped cells with a length of 1–5 μm and a width of 0.4–0.7 μm under an electron microscope, and no flagella were observed (Fig. 6B). As gliding motility is widespread among members of the phylum Bacteroidetes (McBride and Zhu, 2013), all reported genes in Bacteroidetes encoding to gliding motility has been identified in the genome of *Ca*. S. hydrothermale (Table S4). Moreover, the isolate was also observed motile under an optical microscope. According to the above observations, we reported the gliding motility of *Ca*. S. hydrothermale.

After purification, the complete genome of the isolate was further obtained by both Illumina and Nanopore sequencing (see Experimental procedures). The complete genome is a single circular chromosome of 3 266 085 bp with an average GC content of 42.23%, which is quite similar to Bin4 assembled from metagenome (Table S8). The complete genome of the isolate contains two rRNA gene operons and 47 tRNA genes (Table S8). Comparison of the genome of the isolate and Bin4 shows that they belong to the same species, with a 99.67% of 16S rRNA gene identity (aligned length 1509 bp, there are five bases difference besides the sequence of PCR results) and 99.04% of average nucleotide identity (ANI) (Table S9), which are higher than the cut-off of species definition (16S rRNA gene identity >98.6% and ANI >95%) (Konstantinidis and Tiedje, 2005b; Yarza *et al*., 2014). Furthermore, all the

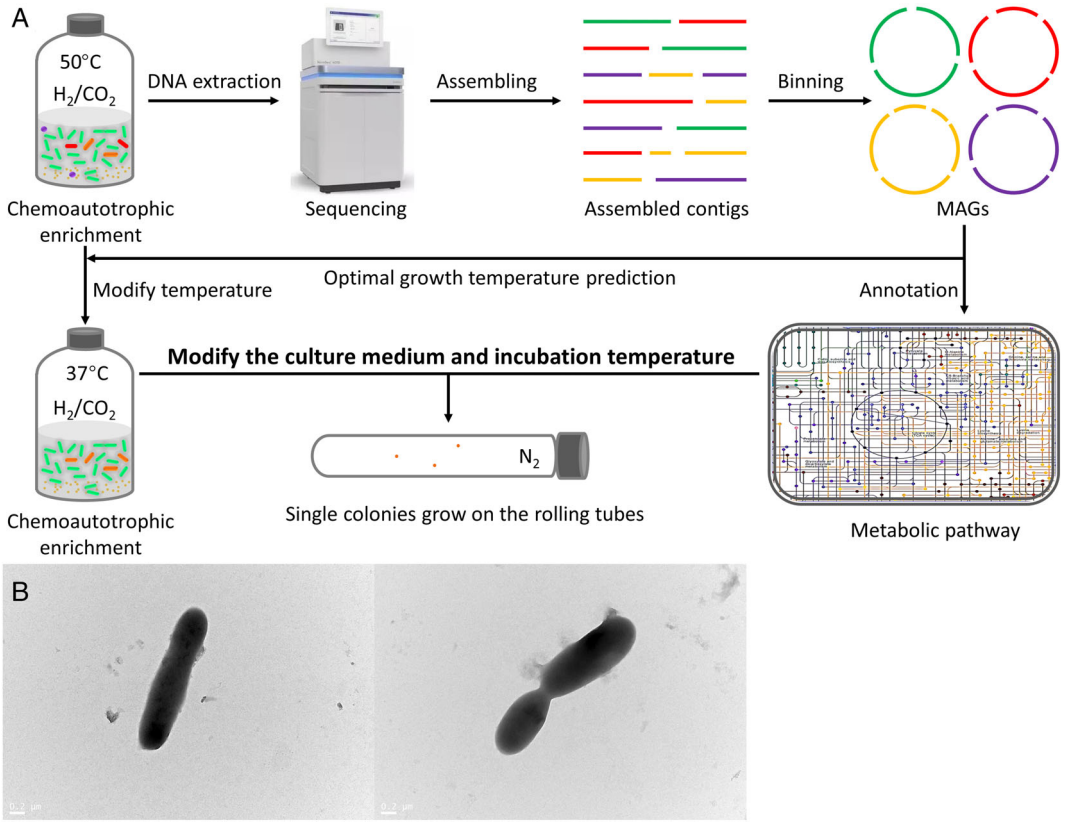

Fig. 6. A. Schematic drawing of the metagenome-guided isolation procedures.
B. Transmission electron micrograph of *Ca*. S. hydrothermale. Cells of *Ca*. S. hydrothermale were rod-shaped cells with a length of 1–5 μm and a width of 0.4–0.7 μm, and no flagella were observed.

functional genes mentioned in this manuscript for Bin4 were confirmed in the complete genome of the isolate.

We further measure the utilization of various carbon sources and electron acceptors in the isolate physiologically. The carbon source utilization experiments showed that separately adding fructose, beef extract, yeast extract and tryptone at a final concentration of 0.2% (wt./vol.) supported the growth of the isolate on the solidified medium in anaerobic rolling tubes. While no growth was observed when D-glucose, sucrose, xylose, xylan, D-cellobiose served as carbon sources. For electron acceptors, the presence of polysulfide significantly stimulated the growth of the isolate (Table S10). During the growth of the isolate, polysulfide was reduced to hydrogen sulfide as detected by the GC–MS (Agilent Technologies 7890B-5977B, see Experimental procedures). N_2O (150 ppm) was measured as another potential electron acceptor. Compared to the negative controls without inoculation, all N_2O was completely consumed by the growth of the isolate as the GC–MS result showed. Whereas the group with NO (100 ppm) supplied seemed to inhibit the growth of the isolate, which had much fewer colonies than the group with polysulfide or N_2O (Table S10). Furthermore, several colonies grew on the medium without any electron acceptors, which demonstrated a fermentation growth capability of the isolate. Taken all together, physiological experiments agreed with the genomic analysis that *Ca*. S. hydrothermale utilizes fructose, polysaccharides (starch), protein-rich carbon sources (beef extract, yeast extract and tryptone) and obtain energy via N_2O reduction, and polysulfide reduction.

Discussion

Carbon metabolism of Ca*. S. hydrothermale*

Bacteroidetes from hydrothermal vents has been reported to contain many genes related to extracellular peptidases and GHs (Zhou *et al*., 2020). Polysaccharide utilization-related proteins SusC and SusD exclusively attributed to Bacteroidetes were identified in the metaproteomes of hydrothermal vent chimneys (Pjevac *et al*., 2018; Meier *et al*., 2019), suggesting that Bacteroidetes were likely responsible for the utilization and recycling of organic carbon compounds supplied by the primary producers (Pjevac *et al*., 2018). In addition,

Bacteroidetes from Guaymas Basin hydrothermal sediments was also reported to have the potential for fatty acid degradation and anaerobic hydrocarbon degradation (Dombrowski *et al*., 2017). Although many metabolic capacities have been reported in Bacteroidetes from hydrothermal vents, previous results were all based on omics, the specific metabolic and ecological insights of *Ca*. Sulfidibacteriales were still unclear. Our discovery that Campylobacterota and Bacteroidetes were co-cultured in chemoautotrophic enrichment indicated that in hydrothermal vents, *Ca*. S. hydrothermale can live on the organic carbon produced by autotrophic microorganisms, surviving without organic matter sedimented from the surface ocean.

Moreover, substrates interactions among autotrophic Campylobacterota and heterotrophic Bacteroidetes were also reported *in situ* in hydrothermal vents and subsurface sediments (Handley *et al*., 2013; Stokke *et al*., 2015). Based on our results, *Ca*. S. hydrothermale may be capable of polysaccharide, protein and fatty acid degradation but not hydrocarbon degradation. This indicates that *Ca*. S. hydrothermale may play an important role in the mineralization of complex organic substrates in hydrothermal vents. *Ca*. S. hydrothermale in the deep-sea anaerobic zone may adopt a 'selfish' carbon utilization strategy similar to that of surface marine Bacteroidetes (Reintjes *et al*., 2019). Bacteroidetes from gut and surface marine have been experimentally identified as carrying out a 'selfish' uptake strategy, which is mechanically mediated by SusC/SusD (Cuskin *et al*., 2015; Reintjes *et al*., 2017; Hehemann *et al*., 2019). In this selfish carbon utilization strategy, high-molecular-weight polysaccharides are first bound by SusD proteins, hydrolysed to low-molecular-weight glycans, transported to the periplasm with an integral membrane SusC-like TonB-dependent transporter, where they are further degraded as monosaccharides and disaccharides by various types of GHs, and then transported into the cell for utilization (Martens *et al*., 2009; Koropatkin *et al*., 2012). The genome analysis of *Ca*. S. hydrothermale identified nine pairs of SusC/SusD and several GHs (Tables S4, S11). The existence of these enzymes indicated that this selfish carbon utilization strategy is also retained in *Ca*. S. hydrothermale from the high-pressure and anaerobic environments. This strategy can maximize the use of carbon sources while requiring little to no production of extracellular hydrolysis products (Reintjes *et al*., 2019); therefore, it can provide an advantage in competition with other microorganisms that secrete GHs extracellularly.

Energy metabolism flexibility of Ca*. S. hydrothermale*

Aerobic respiration produces far more energy than anaerobic respiration and anaerobic fermentation. For this reason, Bacteroidetes living in the surface ocean, where there is sufficient oxygen due to the mixing of ocean currents, prefer to produce energy via aerobic respiration. However, *Ca*. S. hydrothermale lives in various anoxic environments that are rich in sulfide, such as the anaerobic zone of deep-sea hydrothermal vents. Fluctuating oxygen/redox gradients form around deep-sea hydrothermal vents due to the mixing of hydrothermal fluids (rich in reduced substances) and the surrounding seawater (rich in oxygen). Therefore, microorganisms living around hydrothermal fluids are likely to be frequently exposed to both aerobic and anaerobic conditions. In this case, the ability to capture oxygen and utilize various electron acceptors will help microbes obtain more energy and enhance their adaptability. The genomic analysis results suggest that, in order to obtain sufficient energy, *Ca*. S. hydrothermale evolved a variety of energetic pathways to utilize multiple electron acceptors (i.e. O_2, NO, N_2O and polysulfide). At the same time, due to the anaerobic respiration of NO, N_2O and polysulfide, *Ca*. S. hydrothermale played a non-negligible role in N and S cycling *in situ*. For N cycling, N_2O and NO are important products of the ammonia oxidation pathway and denitrification under low-oxygen conditions (Zhu *et al*., 2013). Abundant ammonia-oxidizing archaea and autotrophic and heterotrophic microorganisms with denitrification abilities thrive in deep-sea hydrothermal vents (Nakagawa and Takai, 2008; Wang *et al*., 2009; Sievert and Vetriani, 2012). The N_2O and NO produced by these microbes during metabolism can be an important energy source for *Ca*. S. hydrothermale. NO can be reduced to N_2O by nitric oxide reductase (NorB), and then N_2O is reduced to N_2, catalysed by N_2O reduction enzymes (NosZ). The phylogeny of the NosZ protein has two distinct clades, clade I and clade II (Sanford *et al*., 2012). The half-saturation constant (*K*m) of clade II NosZ for N_2O is much lower than that of clade I, indicating that clade II has a much higher affinity for N_2O and that it determines the N_2O sink capacity in a given environment (Yoon *et al*., 2016). The phylogenetic analysis showed that *Ca*. S. hydrothermale contains clade II NosZ (Fig. S3), which enables cells to utilize trace amounts of N_2O produced by other microbes in hydrothermal vents and to play an important role as N_2O sinks in hydrothermal vents. With regard to S cycling, there is plenty of polysulfide in hydrothermal vents and oxygen-deficient zones in the ocean (e.g. oxygen-minimum zones and the subsurface of marine sediments) (Findlay *et al*., 2019; Jørgensen *et al*., 2019). Polysulfides are supplied mainly by the outflow of hydrothermal vents or formed by the oxidation of sulfides generated by sulfate-reducing bacteria. The genome of *Ca*. S. hydrothermale contains polysulfide reductase (*psrA*), which allows it to use polysulfide to gain energy. This observation also supports the previous hypothesis that the growth of *Ca*. Sulfidibacteriales

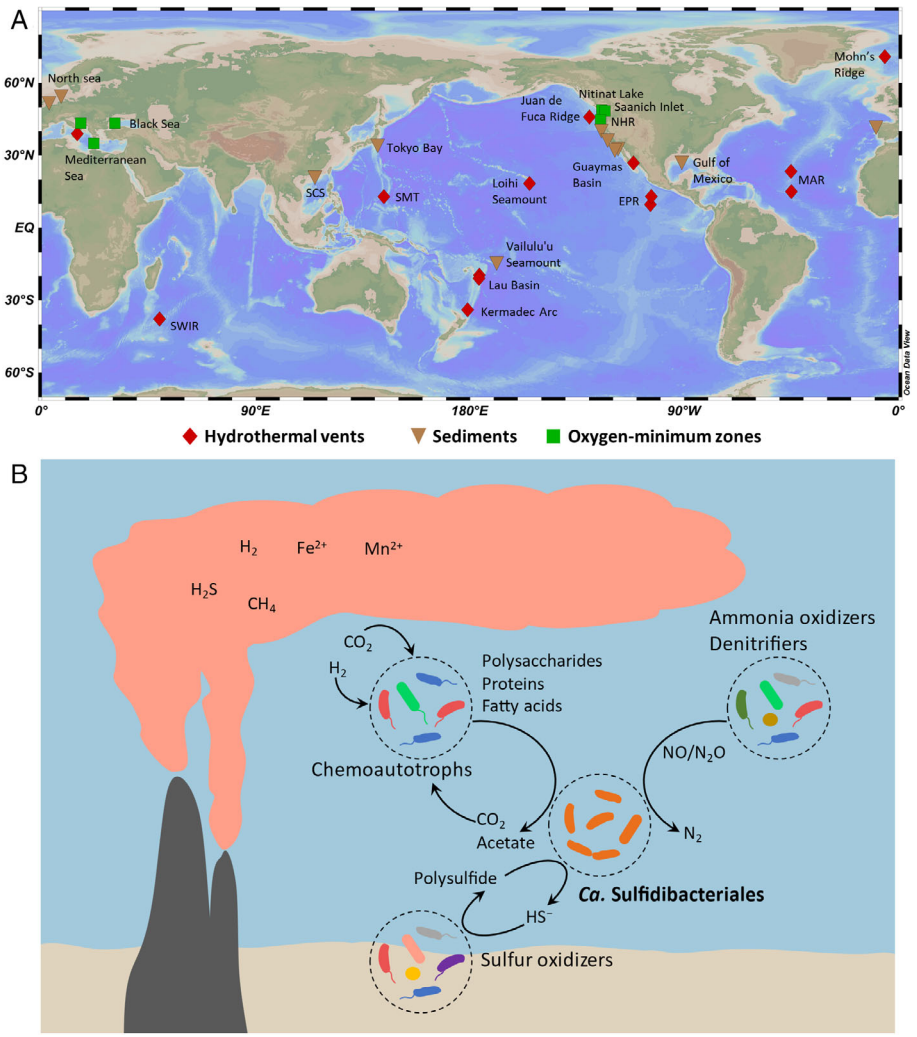

Fig. 7. A. The global distribution of *Ca*. Sulfidibacteriales. *Ca*. Sulfidibacteriales is mainly from sulfidic environments such as inactive sulfides, active hydrothermal vents, oxygen minimum zones and sediments (Table S12). SMT: Southern Mariana Trough; SWIR: Southwest Indian Ridge; SCS: South China Sea; EPR: East Pacific Rise; MAR: Mid-Atlantic Ridge; NHR: North Hydrate Ridge. The map was created using Ocean Data View (version 5.2.0; Schlitzer, Reiner, Ocean Data View, https://odv.awi.de, 2018).
B. Schematic illustration shows the ecological roles of *Ca*. Sulfidibacteriales in hydrothermal vents.

requires reduced sulfur (Sylvan *et al*., 2013). Overall, the flexibility of *Ca*. S. hydrothermale, in terms of electron acceptor utilization, increases its environmental adaptability and is conducive to its ecological radiation in marine anoxic environments.

Ecological potentials of Ca*. Sulfidibacteriales in the hydrothermal vents*

Ca. Sulfidibacteriales are widely distributed in oxygen-deficient zones in the ocean (e.g. hydrothermal vents, oxygen-minimum zones, sediments) (Fig. 7A) and are abundant in hydrothermal vents, especially in inactive chimneys (Sylvan *et al*., 2012; Sylvan *et al*., 2013; Li *et al*., 2017). The limited distribution of *Ca*. Sulfidibacteriales in aerobic conditions indicated the disability for oxygen respiration. The oxygen-respiration related enzyme in *Ca*. S. hydrothermale is only cytochrome bd oxidase (CydA, CydB). It is reported that cytochrome bd has a high affinity for O_2 and is highly expressed under oxygen-limited conditions (Borisov *et al*., 2011). Moreover, *Ca*. S. hydrothermale has the potential of anaerobic respiration using polysulfide, NO, N_2O, thus facilitating *Ca*. S. hydrothermale to colonize oxygen-deficient environments. In contrast, the aa3-type cytochrome *c* oxidase that functions under oxic conditions (Fang *et al*., 2021) is absent in *Ca*. S. hydrothermale, which may constrain *Ca*. S. hydrothermale's ecological distribution in areas with higher oxygen levels. The genome of *Ca*. S. hydrothermale reveals the potential contributions of *Ca*. Sulfidibacteriales to carbon, nitrogen and sulfur cycling in hydrothermal vents (Fig. 7B). As an important heterotrophic decomposer, *Ca*. Sulfidibacteriales may degrade polymers with high molecular weights and attach to particulate organic carbon, which can induce the mineralization of complex organic carbon and particulate organic carbon in hydrothermal vents. As a hot spot for N_2O production in the ocean, hydrothermal vents release a large amount of greenhouse gases during the

processes of denitrification and ammonia oxidation (Lilley *et al*., 1982; Bange and Andreae, 1999; Kawagucci *et al*., 2010). *Ca*. Sulfidibacteriales may play an important role as an N_2O sink to prevent emissions from hydrothermal vents. A large number of sulfur-oxidizing bacteria thrive in hydrothermal vents, and the sulfide produced by *Ca*. Sulfidibacteriales during the sulfur reduction process can be used as an electron donor for sulfur-oxidizing bacteria. At the same time, the elemental sulfur produced by sulfur-oxidizing bacteria can be used as an electron acceptor by *Ca*. Sulfidibacteriales. This high-speed circulation of electron carriers can allow microorganisms in hydrothermal areas to obtain energy more efficiently.

Particle-associated lifestyle of Ca*. S. hydrothermale*

Interestingly, although we obtained single colonies of *Ca*. S. hydrothermale in rolling tubes successfully and quickly (~7 days to observe single colonies), no testable growth was observed when single colonies were transferred to a liquid medium with the same recipe within 60 days of cultivation. Three potential reasons for this phenomenon could be suspected: (i) agar that was used to make solid medium can be used as a carbon source to support the growth of *Ca*. S. hydrothermale; (ii) some substances in the autotrophic enrichment that were transferred with the inoculation in rolling tubes supported the growth of *Ca*. S. hydrothermale, but the amount was quite low when the colonies were transferred to liquid medium; or (iii) *Ca*. S. hydrothermale required a solid surface for growth. To test the potential reasons (i) and (ii), we transferred single colonies in a solid medium to the liquid medium containing a small amount of agar (0.1% wt./vol.) or sterilized autotrophic enrichment medium (10% vol./vol.) for 27 days of cultivation. However, still no growth was observed. Besides, all reported agar-degrading enzymes [α-agarase (EC 3.2.1.158), β-agarase (EC 3.2.1.81), and β-porphyranase (EC 3.2.1.-)] in distinct GH families in the CAZy database (GH16, GH50, GH86, GH96, GH117 and GH118) were not identified in the genome of *Ca*. S. hydrothermale (Table S5). Furthermore, we successfully cultivate the isolate on the rolling tubes replacing agar with gellan gum (1.5% wt./vol.; Gelzan™ CM, Sigma-Aldrich). Then, we excluded (i) and (ii). Therefore, it seems that *Ca*. S. hydrothermale required a solid surface for growth as (iii) mentioned. Bacteroidetes has been reported to be significantly enriched on particles compared to free-living microbial communities in seawaters (Eloe *et al*., 2011; Milici *et al*., 2017), which suggests Bacteroidetes prefers to grow attached to particles (Fernández-Gómez *et al*., 2013). In addition, Bacteroidetes was also reported to perform as an ability of surface adhesion and gliding motility that required contact with a surface (Jarrell and McBride, 2008). All genes encoding in the surface adhesion and gliding motility has been identified in the genome of *Ca*. S. hydrothermale (Table S4). It implies that *Ca*. S. hydrothermale may specialize in a particle-associated lifestyle. However, the case of *Ca*. S. hydrothermale seems special that a stable co-culture of *Ca*. S. hydrothermale were obtained successfully at the first step of chemoautotrophic enrichment in liquid medium. And adding quartz beads in the liquid medium could not resume the growth of the isolate during 30 days of cultivation. These results indicated *Ca*. S. hydrothermale possibly attached to the surface of organic matter or other microbes in liquid medium. Bacteroidetes adhering to the surface of other bacteria have also been observed in the natural hydrothermal environment. Stokke *et al*. (2015) found that in the biofilm of Loki's Castle vent field, Bacteroidetes attached to the cell surface of long filamentous *Sulfurovum* within Campylobacterota and speculated that it could degrade organic polymers produced by the autotrophic Sulfurovum. The cultivation and physiological tests of *Ca*. S. hydrothermale still need a lot of further investigations to figure out the difficulties caused by their particle-associated lifestyle.

In summary, this work provides the first comprehensive genomic insights into the metabolic strategies and potential ecological functions of a previously uncultivated microbial lineage, *Ca*. Sulfidibacteriales, in deep-sea hydrothermal vents. Guided by the metagenomic information, the first representative strain, *Ca*. S. hydrothermale was successfully isolated. This enhanced our confidence in the metagenome-guided isolation of the uncultured microbes. Both isolate and complete genome information of *Ca*. S. hydrothermale laid a foundation for future studies on the physiological characteristics, which will improve our understanding of the real ecological function of this lineage in deep-sea hydrothermal vents.

Experimental procedures

Sample collection

A chimney sample was collected from the L vent (9°46.25′ N, 104°16.74′ W) on the East Pacific Rise on 16 January 2014 (Dive 761) using the deep-sea research submarine ROV Jason II during the R/V Atlantis research cruise AT26-10 (2013/12/27-2014/1/26). The sampling depth was 2528 m. The maximum measured temperature of the fluid in the middle of the black chimney was 231°C. More information about the fluid geochemistry and microbial communities in the chimney walls can be found in Hou *et al*. (2020). The sample was stored immediately upon retrieval in sterile anaerobic tubes, and the headspace of the tubes was filled with pure nitrogen gas

with slight overpressure to prevent the entry of oxygen. The samples were then stored at 4°C until being used for enrichment in the laboratory.

Enrichment procedures

Samples (0.25 g) from the outer layer of the black chimney were initially enriched anaerobically in a chemoautotrophic SME medium (Vetriani *et al*., 2004) containing the following components (per litre): NaCl, 20.0 g; $MgSO_4{\cdot}7H_2O$, 3.5 g; $MgCl_2{\cdot}6H_2O$, 2.75 g; KCl, 0.325 g; KNO_3, 2.0 g; MES, 4.27 g; NaBr, 50.0 mg; H_3BO_3, 15.0 mg; $SrCl_2{\cdot}6H_2O$, 7.5 mg; $(NH_4)_2SO_4$, 10·0 mg; KI, 0.05 mg; $Na_2WO_2{\cdot}2H_2O$, 0.1 mg; $CaCl_2{\cdot}2H_2O$, 0.75 g; KH_2PO_4, 0.5 g; $NiCl_2{\cdot}6H_2O$, 2.0 mg; and resazurin, 1.0 mg. The pH of the medium was adjusted to 6.0. After autoclaving, 1 ml of trace element mixture (Widdel *et al*., 2006), 1 ml of vitamin mixture (Widdel *et al*., 2006), 1 ml of thiamine solution (Widdel *et al*., 2006) and 1 ml of vitamin B12 solution (Widdel *et al*., 2006) were added to 1 L of medium. Then, 50 ml of the medium was divided among 150 ml glass serum bottles and supplemented with 0.5 g of elemental sulfur and 0.5 ml of $Na_2S{\cdot}9H_2O$ (10%, wt./vol.; pH 7.0). The tightly stoppered bottles were pressurized with H_2/CO_2 (80:20; 101 kPa). The enrichment cultures were incubated at 50°C. We obtained the original enrichment in this chemolithotrophic medium and transferred the enriched culture (1% inoculation) to this medium for five rounds.

DNA extraction, metagenome sequencing and data analysis

DNA was extracted following a modified SDS-based DNA extraction method (Natarajan *et al*., 2016). The extracted DNA quality checking and sequencing were conducted by BGI (Shenzhen, China). Paired-end sequencing was performed using a HiSeq X System (Illumina). The raw shotgun sequencing metagenomic reads were trimmed using Sickle v1.33 (https://github.com/najoshi/sickle). Whole-genome *de novo* assemblies were performed using SPAdes v3.14.0 (Nurk *et al*., 2017) with the following parameters: --meta, -k 21,33,55,77,99. Binning of assembled sequences longer than 2 kb was performed by MetaWRAP v1.2.1 (Uritskiy *et al*., 2018) using Binning (--metabat2 --maxbin2 --concoct options), Bin_refinement (-c 50 -x 10 options) and Reassemble_bins modules. The retrieved MAGs were further checked manually using the R package 'mmgenome' v.0.4.1 (Karst *et al*., 2016). Genomic abundance was calculated by aligning the quality-filtered read files from the metagenome with the final MAGs in Bowtie v2.2.8 (Langmead and Salzberg, 2012). The completeness, contamination and strain heterogeneity of the MAGs were then estimated by using CheckM v1.0.7 (Parks *et al*., 2015). tRNA annotation was performed with tRNAscan-SE v1.3.1 (Lowe and Eddy, 1997). The rRNA coding regions (5S, 16S and 23S rRNA) in each genome were identified using both CheckM SSU_finder (Parks *et al*., 2015) and RNAmmer v1.2 (Ussery *et al*., 2007). Protein-coding sequences in the bins were predicted by Prodigal v.2.6.3 (Hyatt *et al*., 2010), and predicted gene functions were annotated with databases including KEGG (BlastKOALA) (Kanehisa *et al*., 2016) and eggNOG-Mapper (Huerta-Cepas *et al*., 2017). The dbCAN webserver (Zhang *et al*., 2018) was used for carbohydrate-active gene identification [cut-offs: HMMER (*E*-value <1e-15, coverage >0.35); DIAMOND (*E*-value <1e-102); Hotpep (frequency >2.6, hits >6)]. Genes encoding proteases and peptidases were identified using DIAMOND (Buchfink *et al*., 2015) against the MEROPS database release 12.0 (cut-offs: *E*-value, 1e-5; sequence identity, 30%) (Rawlings *et al*., 2018). Signal peptide prediction was conducted by the SignalP-5.0 online server (Almagro Armenteros *et al*., 2019). Based on gene annotation, metabolic pathways were constructed for these bins. The average AAIs between homologues in genome pairs were calculated using the AAI calculator with default settings in CompareM v0.0.4 (https://github.com/dparks1134/CompareM). The optimal growth temperature of the enriched strains was predicted based on the MAGs using Tome v1.1 (Li *et al*., 2019). Tome used a collection of optimal growth temperature and proteomes of microorganisms as a training data set to train a machine learning model, this model was in turn used to predict optimal growth temperatures for the uncultured microbes with proteomes as input.

Amplicon sequencing and diversity analyses

The bacterial V4 region of the 16S rRNA gene was amplified by B515F (5′-XXXXXXXXGTGCCAGCMGCCG CGGTAA-3′) with eight-nucleotide key tags for each sample and B806R (5′-GGACTACHVGGGTWTCTAAT-3′) (Caporaso *et al*., 2011); the X region represents the various key tags for each sample. The PCR program was 3 min at 95°C, followed by 35 cycles of 94°C for 40 s, 56°C for 1 min and 72°C for 1 min. The final extension step was 72°C for 7 min. The 50 μl amplification mixture contained 1 μl of each forward and reverse primer, 1 μl template DNA, 5 μl 10× Ex Taq buffer, 0.5 μl ExTaq polymerase (TaKaRa, Japan), 4 μl of 2.5 mM dNTP mix and 37.5 μl ddH_2O. PCR products were purified with an E.Z.N.A. Gel Extraction Kit (OmegaBio-Tek, USA) and sequenced on the MiSeq platform (Illumina, USA) according to the manufacturer's instructions.

Data analysis of the 16S rRNA MiSeq sequences was performed using the QIIME version 1.9.1 software pipeline (Caporaso *et al*., 2010) and the QIIME-compatible

version of the SILVA-132 database (Quast *et al*., 2013) for template-based alignment and taxonomic assignment. Assembled reads that passed the chimaera check were clustered into *de novo* operational taxonomic units (OTUs) at a cut-off of 97% sequence similarity.

Phylogenetic analyses

For the 16S rRNA gene tree, the 16S gene sequences were aligned using SINA v1.2.11 (Pruesse *et al*., 2012) with default parameters, and the full alignment was stripped of columns containing 50% or more gaps with a Perl script. The maximum-likelihood phylogeny of the 16S rRNA gene tree was inferred by IQ-TREE v1.6.6 (Nguyen *et al*., 2014) with the '-MFP -bb 1000' options for best-fit model selection and an ultrafast bootstrap value of 1000. The reference sequences of Bacteroidetes VC2.1 Bac22 were downloaded from the Silva database (Silva 132), sequences smaller than 1400 bp were filtered out and OTUs were obtained from the remaining sequences at a cut-off of 97%. These representative OTU sequences were included in the phylogenetic tree. For the phylogenomic analysis, the protein sequences of 43 conserved marker genes (Table S13) used by CheckM (Parks *et al*., 2015) were extracted and aligned in CheckM v1.0.7 and filtered with trimAl v1.4.rev15 (Capella-Gutiérrez *et al*., 2009) with the parameter -automated1. Then, the phylogenetic tree was constructed with IQ-Tree v1.6.6 (Nguyen *et al*., 2014) using the best-fitting protein model predicted in ModelFinder with the parameters '-MFP -bb 1000'. For the phylogenetic tree of nitrous-oxide reductase (NosZ), sequences were aligned using MAFFT v7.313 (Katoh and Standley, 2013) with the parameters --localpair --maxiterate 1000, and the alignment was trimmed with trimAl v1.4.rev15 with the parameter -automated1. Then, the phylogenetic tree was constructed by IQ-Tree v1.6.6 with the parameters '-MFP -bb 1000'. All trees were visualized using iTOL (Letunic and Bork, 2019) online software.

Metagenome-guided isolation

Based on the predicted optimal growth temperature, the chemoautotrophic community enriched at 50°C was transferred to 37°C conditions in the same chemoautotrophic medium. After positive growth was achieved (7 days), chemoautotrophic enrichment was spread on rolling tubes containing solid mSME medium (1.5% agar). The mSME medium was made up of SME medium with nitrate removed, 3 g L^{-1} starch as the sole carbon source, 0.5 g L^{-1} ammonium sulfate as nitrogen source and 0.1 g L^{-1} yeast extract, after autoclave, added 1% (vol./vol.) polysulfide solution (Matsumi *et al*., 2007). The inoculated rolling tubes were anaerobically incubated at 37°C for 7 days. Single colonies were independently picked in an anaerobic chamber. The purity of the strain was confirmed by transmission electron microscopy (TEM) and sequencing of the 16S rRNA gene of the single colonies (with the primers B27F/U1492R). And the strain has been deposited in the Marine Culture Collection of China (www.mccc.org.cn; accession number: MCCC 1K06756).

TEM and gilding motility observation

For TEM, cells were fixed in 4% formaldehyde for 2 h at room temperature, harvested at 3000*g* for 5 min, and washed with PBS solution three times. The fixed cells were placed on copper grids and dried for 30 min at room temperature, and the prepared samples were observed with a transmission electron microscope (FEI Tecnai G2 Spirit Biotwin).

To observe gilding motility, *Ca*. S. hydrothermale was grown anaerobically on mSME agar in a rolling tube. Colonies were suspended in SME medium in an anaerobic chamber and examined for motility in the presence of atmospheric levels of O_2. Cells were observed in wet mount using an Olympus BX63 microscope equipped with an Olympus DP74 camera under room temperature.

Complete genome sequencing and analysis

Pure-cultured colonies in the rolling tubes were washed off using SME medium and then harvested at 10 000*g* for 10 min. Genomic DNA of the isolate was extracted according to a modified SDS-based DNA extraction method (Natarajan *et al*., 2016). Genome sequencing was then performed on both Illumina NovaSeq (2 × 250 bp paired-end) and Oxford Nanopore Technology (ONT) PromethION platform. For the Illumina sequencing, the raw reads were trimmed using fastp v0.20.1 (Chen *et al*., 2018) to remove low-quality reads and adapters, yielding 3 394 292 reads in total. For the ONT sequencing, adapters were removed from the raw data by Porechop v0.2.4 (https://github.com/rrwick/Porechop), then the retained sequence was filtered by Filtlong 0.2.1 (https://github.com/rrwick/Filtlong) with the following parameters: --min_length 2000 --min_mean_q 7 --target_bases 500000000. The clean data are about 500 Mbp with 14 506 reads (average length, 34 468 bp). Hybrid assembly of Illumina and ONT reads was performed using Unicycler v0.4.8 (Wick *et al*., 2017). Annotation of tRNA was performed with tRNAscan-SE v1.3.1 (Lowe and Eddy, 1997). The rRNA coding regions (5S, 16S and 23S rRNA) were identified using RNAmmer v1.2 (Ussery *et al*., 2007). Protein-coding sequences were predicted by Prodigal v.2.6.3 (Hyatt *et al*., 2010), and

predicted gene functions were annotated with databases including KEGG (BlastKOALA) (Kanehisa *et al*., 2016) and eggNOG-Mapper v2.0 (Huerta-Cepas *et al*., 2017). ANI of the complete genome was calculated by the JSpeciesWS webserver (Richter *et al*., 2016).

Physiological measurements

To test carbon source utilization, various carbon sources at a final concentration of 0.2% (wt./vol.) were added into a basal mSME medium (without starch) and supplemented with 1% (vol./vol.) polysulfide solution, then solidified with 1.5% agar in rolling tubes. The tested carbon sources were as follows: D-glucose, D-fructose, sucrose, xylose, xylan, D-cellobiose, beef extract, yeast extract, tryptone. All tests were performed in duplicate and incubated anaerobically at 45°C for 18 days.

To examine the ability of the isolate to grow with different electron accepters, solidified mSME medium was prepared in rolling tubes. The medium supplemented with $Na_2S{\cdot}9H_2O$ (10%, wt./vol.; pH 7.0) was used to test the fermentation growth ability; the medium supplemented with 1% (vol./vol.) polysulfide was used to test the polysulfide utilization; the medium supplemented with polysulfide by adding extra N_2O (150 ppm) or NO (100 ppm) was used to test the utilization as extra electron acceptors for N_2O or NO (Table S10). All tests were performed in triplicate and incubated anaerobically at 45°C for 2 weeks. For N_2O and NO groups, three rolling tubes without inoculation were set as negative controls.

N_2O and H_2S concentrations were measured by GC–MS (Agilent Technologies 7890B-5977B). The GC–MS was equipped with a Pora PLOT Q column (25 m × 0.32 mm × 10 μm) with ultrahigh purity helium (99.999%) as the carrier gas at a flow rate of 1.5 ml min^{-1}. The injector temperature was set as 240 °C. The column oven temperature program was set as follows: hold at 40°C for 5 min, ramp to 200°C at 20°C min^{-1}. MS analysis was carried out with 70 eV as ionization energy and over a mass-to-charge ratio (*m*/*z*) range of 10–200. The MS source and quadrupole were held at 230°C and 150°C respectively.

Data accession

Metagenomic sequence reads, metagenome-assembled genomes and amplicon sequencing datasets have been deposited at NCBI under Bioproject PRJNA716772. The complete genome sequence of *Ca*. S. hydrothermale was deposited under accession number CP083760.

Acknowledgements

We thank the crew of the R/V Atlantis and the ROV Jason II during cruise AT26-10 for their assistance in obtaining the samples for this study. We thank Yongxin Lv and Jiahua Wang for the support and advice related to the bioinformatic analysis. This study was financially supported by the National Natural Science Foundation of China (grant numbers 41921006, 41530967 and 41776173). The research expedition was funded by the US National Science Foundation Dimensions of Biodiversity Grant.

References

Alain, K., Olagnon, M., Desbruyères, D., Pagé, A., Barbier, G., Juniper, S.K., *et al*. (2002) Phylogenetic characterization of the bacterial assemblage associated with mucous secretions of the hydrothermal vent polychaete Paralvinella palmiformis. *FEMS Microbiol Ecol* **42**: 463–476.

Alain, K., Zbinden, M., Le Bris, N., Lesongeur, F., Quérellou, J., Gaill, F., and Cambon-Bonavita, M.-A. (2004) Early steps in microbial colonization processes at deep-sea hydrothermal vents. *Environ Microbiol* **6**: 227–241.

Almagro Armenteros, J.J., Tsirigos, K.D., Sønderby, C.K., Petersen, T.N., Winther, O., Brunak, S., *et al*. (2019) SignalP 5.0 improves signal peptide predictions using deep neural networks. *Nat Biotechnol* **37**: 420–423.

Bange, H.W., and Andreae, M.O. (1999) Nitrous oxide in the deep waters of the world's oceans. *Global Biogeochem Cycles* **13**: 1127–1135.

Borisov, V.B., Gennis, R.B., Hemp, J., and Verkhovsky, M.I. (2011) The cytochrome bd respiratory oxygen reductases. *Biochim Biophys Acta* **1807**: 1398–1413.

Bowers, R.M., Kyrpides, N.C., Stepanauskas, R., Harmon-Smith, M., Doud, D., Reddy, T.B.K., *et al*. (2017) Minimum information about a single amplified genome (MISAG) and a metagenome-assembled genome (MIMAG) of bacteria and archaea. *Nat Biotechnol* **35**: 725–731.

Brown, K., Tegoni, M., Prudêncio, M., Pereira, A.S., Besson, S., Moura, J.J., *et al*. (2000) A novel type of catalytic copper cluster in nitrous oxide reductase. *Nat Struct Biol* **7**: 191–195.

Buchfink, B., Xie, C., and Huson, D.H. (2015) Fast and sensitive protein alignment using DIAMOND. *Nat Methods* **12**: 59–60.

Cao, J., Birien, T., Gayet, N., Huang, Z., Shao, Z., Jebbar, M., and Alain, K. (2017) Desulfurobacterium indicum sp. nov., a thermophilic sulfur-reducing bacterium from the Indian Ocean. *Int J Syst Evol Microbiol* **67**: 1665–1668.

Capella-Gutiérrez, S., Silla-Martínez, J.M., and Gabaldón, T. (2009) trimAl: a tool for automated alignment trimming in large-scale phylogenetic analyses. *Bioinformatics* **25**: 1972–1973.

Caporaso, J.G., Kuczynski, J., Stombaugh, J., Bittinger, K., Bushman, F.D., Costello, E.K., *et al*. (2010) QIIME allows analysis of high-throughput community sequencing data. *Nat Methods* **7**: 335–336.

Caporaso, J.G., Lauber, C.L., Walters, W.A., Berg-Lyons, D., Lozupone, C.A., Turnbaugh, P.J., *et al*. (2011) Global patterns of 16S rRNA diversity at a depth of millions of sequences per sample. *Proc Natl Acad Sci USA* **108**: 4516–4522.

Chen, S., Zhou, Y., Chen, Y., and Gu, J. (2018) fastp: an ultra-fast all-in-one FASTQ preprocessor. *Bioinformatics* **34**: i884–i890.

Chen, S.-C., Sun, G.-X., Yan, Y., Konstantinidis, K.T., Zhang, S.-Y., Deng, Y., *et al*. (2020) The great oxidation event expanded the genetic repertoire of arsenic metabolism and cycling. *Proc Natl Acad Sci USA* **117**: 10414–10421.

Cuskin, F., Lowe, E.C., Temple, M.J., Zhu, Y., Cameron, E. A., Pudlo, N.A., *et al*. (2015) Human gut Bacteroidetes can utilize yeast mannan through a selfish mechanism. *Nature* **517**: 165–169.

DeLong, E.F. (1992) Archaea in coastal marine environments. *Proc Natl Acad Sci U S A* **89**: 5685–5689.

Dhillon, A., Teske, A., Dillon, J., Stahl, D.A., and Sogin, M.L. (2003) Molecular characterization of sulfate-reducing bacteria in the Guaymas Basin. *Appl Environ Microbiol* **69**: 2765–2772.

Dombrowski, N., Seitz, K.W., Teske, A.P., and Baker, B.J. (2017) Genomic insights into potential interdependencies in microbial hydrocarbon and nutrient cycling in hydrothermal sediments. *Microbiome* **5**: 106.

Doud, D.F.R., Bowers, R.M., Schulz, F., De Raad, M., Deng, K., Tarver, A., *et al*. (2019) Function-driven single-cell genomics uncovers cellulose-degrading bacteria from the rare biosphere. *ISME J* **14**: 659–675.

Eloe, E.A., Shulse, C.N., Fadrosh, D.W., Williamson, S.J., Allen, E.E., and Bartlett, D.H. (2011) Compositional differences in particle-associated and free-living microbial assemblages from an extreme deep-ocean environment. *Environ Microbiol Rep* **3**: 449–458.

Fang, Y., Yuan, Y., Liu, J., Wu, G., Yang, J., Hua, Z., *et al*. (2021) Casting light on the adaptation mechanisms and evolutionary history of the widespread Sumerlaeota. *mBio* **12**: e00350-00321.

Fernández-Gómez, B., Richter, M., Schüler, M., Pinhassi, J., Acinas, S.G., González, J.M., and Pedrós-Alió, C. (2013) Ecology of marine Bacteroidetes: a comparative genomics approach. *ISME J* **7**: 1026–1037.

Findlay, A.J., Estes, E.R., Gartman, A., Yücel, M., Kamyshny, A., and Luther, G.W. (2019) Iron and sulfide nanoparticle formation and transport in nascent hydrothermal vent plumes. *Nat Commun* **10**: 1597.

Giuffrè, A., Borisov, V.B., Arese, M., Sarti, P., and Forte, E. (2014) Cytochrome bd oxidase and bacterial tolerance to oxidative and nitrosative stress. *Biochim Biophys Acta* **1837**: 1178–1187.

Handley, K.M., VerBerkmoes, N.C., Steefel, C.I., Williams, K.H., Sharon, I., Miller, C.S., *et al*. (2013) Biostimulation induces syntrophic interactions that impact C, S and N cycling in a sediment microbial community. *ISME J* **7**: 800–816.

Hehemann, J.-H., Reintjes, G., Klassen, L., Smith, A.D., Ndeh, D., Arnosti, C., *et al*. (2019) Single cell fluorescence imaging of glycan uptake by intestinal bacteria. *ISME J* **13**: 1883–1889.

Hino, T., Matsumoto, Y., Nagano, S., Sugimoto, H., Fukumori, Y., Murata, T., *et al*. (2010) Structural basis of biological N_2O generation by bacterial nitric oxide reductase. *Science* **330**: 1666–1670.

Hou, J., Sievert, S.M., Wang, Y., Seewald, J.S., Natarajan, V.P., Wang, F., and Xiao, X. (2020) Microbial succession during the transition from active to inactive stages of deep-sea hydrothermal vent sulfide chimneys. *Microbiome* **8**: 102.

Huerta-Cepas, J., Forslund, K., Coelho, L.P., Szklarczyk, D., Jensen, L.J., von Mering, C., and Bork, P. (2017) Fast genome-wide functional annotation through orthology assignment by eggNOG-mapper. *Mol Biol Evol* **34**: 2115–2122.

Hugenholtz, P., Skarshewski, A., and Parks, D.H. (2016) Genome-based microbial taxonomy coming of age. *Cold Spring Harb Perspect Biol* **8**: a018085.

Hyatt, D., Chen, G.-L., LoCascio, P.F., Land, M.L., Larimer, F.W., and Hauser, L.J. (2010) Prodigal: prokaryotic gene recognition and translation initiation site identification. *BMC Bioinformatics* **11**: 119.

Jarrell, K.F., and McBride, M.J. (2008) The surprisingly diverse ways that prokaryotes move. *Nat Rev Microbiol* **6**: 466–476.

Jørgensen, B.B., Findlay, A.J., and Pellerin, A. (2019) The biogeochemical sulfur cycle of marine sediments. *Front Microbiol* **10**: 849.

Jormakka, M., Yokoyama, K., Yano, T., Tamakoshi, M., Akimoto, S., Shimamura, T., *et al*. (2008) Molecular mechanism of energy conservation in polysulfide respiration. *Nat Struct Mol Biol* **15**: 730–737.

Kabisch, A., Otto, A., König, S., Becher, D., Albrecht, D., Schüler, M., *et al*. (2014) Functional characterization of polysaccharide utilization loci in the marine Bacteroidetes '*Gramella forsetii*' KT0803. *ISME J* **8**: 1492–1502.

Kanehisa, M., Sato, Y., and Morishima, K. (2016) BlastKOALA and GhostKOALA: KEGG tools for functional characterization of genome and metagenome sequences. *J Mol Biol* **428**: 726–731.

Karst, S.M., Kirkegaard, R.H., and Albertsen, M. (2016) mmgenome: a toolbox for reproducible genome extraction from metagenomes. *bioRxiv*: 059121.

Kato, S., Ikehata, K., Shibuya, T., Urabe, T., Ohkuma, M., and Yamagishi, A. (2015) Potential for biogeochemical cycling of sulfur, iron and carbon within massive sulfide deposits below the seafloor. *Environ Microbiol* **17**: 1817–1835.

Katoh, K., and Standley, D.M. (2013) MAFFT multiple sequence alignment software version 7: improvements in performance and usability. *Mol Biol Evol* **30**: 772–780.

Kawagucci, S., Shirai, K., Lan, T.F., Takahata, N., Tsunogai, U., Sano, Y., and Gamo, T. (2010) Gas geochemical characteristics of hydrothermal plumes at the HAKUREI and JADE vent sites, the Izena Cauldron, Okinawa Trough. *Geochem J* **44**: 507–518.

Kirchman, D.L. (2002) The ecology of Cytophaga–Flavobacteria in aquatic environments. *FEMS Microbiol Ecol* **39**: 91–100.

Konstantinidis, K.T., and Tiedje, J.M. (2005a) Towards a genome-based taxonomy for prokaryotes. *J Bacteriol* **187**: 6258–6264.

Konstantinidis, K.T., and Tiedje, J.M. (2005b) Genomic insights that advance the species definition for prokaryotes. *Proc Natl Acad Sci U S A* **102**: 2567–2572.

Koropatkin, N.M., Cameron, E.A., and Martens, E.C. (2012) How glycan metabolism shapes the human gut microbiota. *Nat Rev Microbiol* **10**: 323–335.

Krüger, K., Chafee, M., Ben Francis, T., Glavina del Rio, T., Becher, D., Schweder, T., *et al*. (2019) In marine Bacteroidetes the bulk of glycan degradation during algae blooms is mediated by few clades using a restricted set of genes. *ISME J* **13**: 2800–2816.

Langmead, B., and Salzberg, S.L. (2012) Fast gapped-read alignment with Bowtie 2. *Nat Methods* **9**: 357–359.

Lanzén, A., Jørgensen, S.L., Bengtsson, M.M., Jonassen, I., Øvreås, L., and Urich, T. (2011) Exploring the composition and diversity of microbial communities at the Jan Mayen hydrothermal vent field using RNA and DNA. *FEMS Microbiol Ecol* **77**: 577–589.

Letunic, I., and Bork, P. (2019) Interactive tree of life (iTOL) v4: recent updates and new developments. *Nucleic Acids Res* **47**: W256–W259.

Li, G., Rabe, K.S., Nielsen, J., and Engqvist, M.K.M. (2019) Machine learning applied to predicting microorganism growth temperatures and enzyme catalytic optima. *ACS Synth Biol* **8**: 1411–1420.

Li, J., Cui, J., Yang, Q., Cui, G., Wei, B., Wu, Z., *et al*. (2017) Oxidative weathering and microbial diversity of an inactive seafloor hydrothermal sulfide chimney. *Front Microbiol* **8**: 1378.

Lilley, M.D., de Angelis, M.A., and Gordon, L.I. (1982) CH_4, H_2, CO and N_2O in submarine hydrothermal vent waters. *Nature* **300**: 48–50.

Lowe, T.M., and Eddy, S.R. (1997) tRNAscan-SE: a program for improved detection of transfer RNA genes in genomic sequence. *Nucleic Acids Res* **25**: 955–964.

Ma, K., Schicho, R.N., Kelly, R.M., and Adams, M.W. (1993) Hydrogenase of the hyperthermophile Pyrococcus furiosus is an elemental sulfur reductase or sulfhydrogenase: evidence for a sulfur-reducing hydrogenase ancestor. *Proc Natl Acad Sci USA* **90**: 5341–5344.

Marcia, M., Ermler, U., Peng, G., and Michel, H. (2009) The structure of Aquifex aeolicus sulfide:quinone oxidoreductase, a basis to understand sulfide detoxification and respiration. *Proc Natl Acad Sci USA* **106**: 9625–9630.

Martens, E.C., Koropatkin, N.M., Smith, T.J., and Gordon, J. I. (2009) Complex glycan catabolism by the human gut microbiota: the Bacteroidetes Sus-like paradigm. *J Biol Chem* **284**: 24673–24677.

Matsumi, R., Manabe, K., Fukui, T., Atomi, H., and Imanaka, T. (2007) Disruption of a sugar transporter gene cluster in a hyperthermophilic archaeon using a host-marker system based on antibiotic resistance. *J Bacteriol* **189**: 2683–2691.

McBride, M.J., and Zhu, Y. (2013) Gliding motility and Por secretion system genes are widespread among members of the phylum bacteroidetes. *J Bacteriol* **195**: 270–278.

Meier, D.V., Pjevac, P., Bach, W., Markert, S., Schweder, T., Jamieson, J., *et al*. (2019) Microbial metal-sulfide oxidation in inactive hydrothermal vent chimneys suggested by metagenomic and metaproteomic analyses. *Environ Microbiol* **21**: 682–701.

Meyer, J.L., Akerman, N.H., Proskurowski, G., and Huber, J. A. (2013) Microbiological characterization of post-eruption 'snowblower' vents at axial seamount, Juan de Fuca Ridge. *Front Microbiol* **4**: 153.

Milici, M., Vital, M., Tomasch, J., Badewien, T.H., Giebel, H.-A., Plumeier, I., *et al*. (2017) Diversity and community composition of particle-associated and free-living bacteria in mesopelagic and bathypelagic Southern Ocean water masses: evidence of dispersal limitation in the Bransfield Strait. *Limnol Oceanogr* **62**: 1080–1095.

Mino, S., Shiotani, T., Nakagawa, S., Takai, K., and Sawabe, T. (2021) Hydrogenimonas urashimensis sp. nov., a hydrogen-oxidizing chemolithoautotroph isolated from a deep-sea hydrothermal vent in the Southern Mariana Trough. *Syst Appl Microbiol* **44**: 126170.

Miroshnichenko, M.L., Kolganova, T.V., Spring, S., Chernyh, N., and Bonch-Osmolovskaya, E.A. (2010) Caldithrix palaeochoryensis sp. nov., a thermophilic, anaerobic, chemo-organotrophic bacterium from a geothermally heated sediment, and emended description of the genus Caldithrix. *Int J Syst Evol Microbiol* **60**: 2120–2123.

Mori, K., Kakegawa, T., Higashi, Y., Nakamura, K.-I., Maruyama, A., and Hanada, S. (2004) Oceanithermus desulfurans sp. nov., a novel thermophilic, sulfur-reducing bacterium isolated from a sulfide chimney in Suiyo Seamount. *Int J Syst Evol Microbiol* **54**: 1561–1566.

Nakagawa, S., and Takai, K. (2008) Deep-sea vent chemoautotrophs: diversity, biochemistry and ecological significance. *FEMS Microbiol Ecol* **65**: 1–14.

Natarajan, V.P., Zhang, X., Morono, Y., Inagaki, F., and Wang, F. (2016) A modified SDS-based DNA extraction method for high quality environmental DNA from seafloor environments. *Front Microbiol* **7**: 986.

Nguyen, L.-T., Schmidt, H.A., von Haeseler, A., and Minh, B. Q. (2014) IQ-TREE: a fast and effective stochastic algorithm for estimating maximum-likelihood phylogenies. *Mol Biol Evol* **32**: 268–274.

Nurk, S., Meleshko, D., Korobeynikov, A., and Pevzner, P.A. (2017) metaSPAdes: a new versatile metagenomic assembler. *Genome Res* **27**: 824–834.

Parks, D.H., Imelfort, M., Skennerton, C.T., Hugenholtz, P., and Tyson, G.W. (2015) CheckM: assessing the quality of microbial genomes recovered from isolates, single cells, and metagenomes. *Genome Res* **25**: 1043–1055.

Patwardhan, S., Smedile, F., Giovannelli, D., and Vetriani, C. (2020) Metaproteogenomic profiling of chemosynthetic microbial biofilms reveals metabolic flexibility during colonization of a shallow-water gas vent. *bioRxiv*: 340729.

Pjevac, P., Meier, D.V., Markert, S., Hentschker, C., Schweder, T., Becher, D., *et al*. (2018) Metaproteogenomic profiling of microbial communities colonizing actively venting hydrothermal chimneys. *Front Microbiol* **9**: 680.

Pommier, T., Canbäck, B., Riemann, L., Boström, K.H., Simu, K., Lundberg, P., *et al*. (2007) Global patterns of diversity and community structure in marine bacterioplankton. *Mol Ecol* **16**: 867–880.

Pruesse, E., Peplies, J., and Glöckner, F.O. (2012) SINA: accurate high-throughput multiple sequence alignment of ribosomal RNA genes. *Bioinformatics* **28**: 1823–1829.

Quast, C., Pruesse, E., Yilmaz, P., Gerken, J., Schweer, T., Yarza, P., *et al*. (2013) The SILVA ribosomal RNA gene database project: improved data processing and web-based tools. *Nucleic Acids Res* **41**: D590–D596.

Rawlings, N.D., Barrett, A.J., Thomas, P.D., Huang, X., Bateman, A., and Finn, R.D. (2018) The MEROPS database of proteolytic enzymes, their substrates and inhibitors in 2017 and a comparison with peptidases in the PANTHER database. *Nucleic Acids Res* **46**: D624–D632.

Reintjes, G., Arnosti, C., Fuchs, B., and Amann, R. (2019) Selfish, sharing and scavenging bacteria in the Atlantic Ocean: a biogeographical study of bacterial substrate utilisation. *ISME J* **13**: 1119–1132.

Reintjes, G., Arnosti, C., Fuchs, B.M., and Amann, R. (2017) An alternative polysaccharide uptake mechanism of marine bacteria. *ISME J* **11**: 1640–1650.

Reysenbach, A.-L., Longnecker, K., and Kirshtein, J. (2000) Novel bacterial and archaeal lineages from an in situ growth chamber deployed at a mid-Atlantic ridge hydrothermal vent. *Appl Environ Microbiol* **66**: 3798–3806.

Richter, M., Rosselló-Móra, R., Oliver Glöckner, F., and Peplies, J. (2016) JSpeciesWS: a web server for prokaryotic species circumscription based on pairwise genome comparison. *Bioinformatics* **32**: 929–931.

Sanford, R.A., Wagner, D.D., Wu, Q., Chee-Sanford, J.C., Thomas, S.H., Cruz-García, C., *et al*. (2012) Unexpected nondenitrifier nitrous oxide reductase gene diversity and abundance in soils. *Proc Natl Acad Sci USA* **109**: 19709–19714.

Sievert, S., and Vetriani, C. (2012) Chemoautotrophy at deep-sea vents: past, present, and future. *Oceanography* **25**: 218–233.

Sievert, S.M., Kuever, J., and Muyzer, G. (2000) Identification of 16S ribosomal DNA-defined bacterial populations at a shallow submarine hydrothermal vent near Milos Island (Greece). *Appl Environ Microbiol* **66**: 3102–3109.

Steinle, L., Knittel, K., Felber, N., Casalino, C., de Lange, G., Tessarolo, C., *et al*. (2018) Life on the edge: active microbial communities in the Kryos MgCl2-brine basin at very low water activity. *ISME J* **12**: 1414–1426.

Stokke, R., Dahle, H., Roalkvam, I., Wissuwa, J., Daae, F.L., Tooming-Klunderud, A., *et al*. (2015) Functional interactions among filamentous Epsilonproteobacteria and Bacteroidetes in a deep-sea hydrothermal vent biofilm. *Environ Microbiol* **17**: 4063–4077.

Suter, E.A., Pachiadaki, M., Taylor, G.T., Astor, Y., and Edgcomb, V.P. (2018) Free-living chemoautotrophic and particle-attached heterotrophic prokaryotes dominate microbial assemblages along a pelagic redox gradient. *Environ Microbiol* **20**: 693–712.

Sylvan, J.B., Sia, T.Y., Haddad, A.G., Briscoe, L.J., Toner, B.M., Girguis, P.R., and Edwards, K.J. (2013) Low temperature geomicrobiology follows host rock composition along a geochemical gradient in Lau Basin. *Front Microbiol* **4**: 61.

Sylvan, J.B., Toner, B.M., and Edwards, K.J. (2012) Life and death of deep-sea vents: bacterial diversity and ecosystem succession on inactive hydrothermal sulfides. *mBio* **3**: e00279-00211.

Teske, A., Hinrichs, K.-U., Edgcomb, V., de Vera Gomez, A., Kysela, D., Sylva, S.P., *et al*. (2002) Microbial diversity of hydrothermal sediments in the Guaymas Basin: evidence for anaerobic Methanotrophic communities. *Appl Environ Microbiol* **68**: 1994–2007.

Thorup, C., Schramm, A., Findlay, A.J., Finster, K.W., and Schreiber, L. (2017) Disguised as a sulfate reducer: growth of the Deltaproteobacterium Desulfurivibrio alkaliphilus by sulfide oxidation with nitrate. *mBio* **8**: e00671-00617.

Unfried, F., Becker, S., Robb, C.S., Hehemann, J.-H., Markert, S., Heiden, S.E., *et al*. (2018) Adaptive mechanisms that provide competitive advantages to marine bacteroidetes during microalgal blooms. *ISME J* **12**: 2894–2906.

Uritskiy, G.V., DiRuggiero, J., and Taylor, J. (2018) MetaWRAP—a flexible pipeline for genome-resolved metagenomic data analysis. *Microbiome* **6**: 158.

Ussery, D.W., Rødland, E.A., Stærfeldt, H.-H., Hallin, P., Rognes, T., and Lagesen, K. (2007) RNAmmer: consistent and rapid annotation of ribosomal RNA genes. *Nucleic Acids Res* **35**: 3100–3108.

Vetriani, C., Speck, M.D., Ellor, S.V., Lutz, R.A., and Starovoytov, V. (2004) *Thermovibrio ammonificans* sp. nov., a thermophilic, chemolithotrophic, nitrate-ammonifying bacterium from deep-sea hydrothermal vents. *Int J Syst Evol Microbiol* **54**: 175–181.

Waite, D.W., Vanwonterghem, I., Rinke, C., Parks, D.H., Zhang, Y., Takai, K., *et al*. (2017) Comparative genomic analysis of the class Epsilonproteobacteria and proposed reclassification to Epsilonbacteraeota (phyl. nov.). *Front Microbiol* **8**: 682.

Walsh, D.A., Zaikova, E., Howes, C.G., Song, Y.C., Wright, J.J., Tringe, S.G., *et al*. (2009) Metagenome of a versatile chemolithoautotroph from expanding oceanic dead zones. *Science* **326**: 578–582.

Wang, S., Xiao, X., Jiang, L., Peng, X., Zhou, H., Meng, J., and Wang, F. (2009) Diversity and abundance of ammonia-oxidizing archaea in hydrothermal vent chimneys of the Juan de Fuca Ridge. *Appl Environ Microbiol* **75**: 4216–4220.

Wick, R.R., Judd, L.M., Gorrie, C.L., and Holt, K.E. (2017) Unicycler: resolving bacterial genome assemblies from short and long sequencing reads. *PLoS Comput Biol* **13**: e1005595.

Widdel, F., Boetius, A., and Rabus, R. (2006) Anaerobic biodegradation of hydrocarbons including methane. In *The Prokaryotes: Volume 2: Ecophysiology and Biochemistry*, Dworkin, M., Falkow, S., Rosenberg, E., Schleifer, K.-H., and Stackebrandt, E. (eds). Springer New York: New York, NY, pp. 1028–1049.

Wright, J.J., Konwar, K.M., and Hallam, S.J. (2012) Microbial ecology of expanding oxygen minimum zones. *Nat Rev Microbiol* **10**: 381–394.

Yarza, P., Yilmaz, P., Pruesse, E., Glöckner, F.O., Ludwig, W., Schleifer, K.-H., *et al*. (2014) Uniting the classification of cultured and uncultured bacteria and archaea using 16S rRNA gene sequences. *Nat Rev Microbiol* **12**: 635–645.

Yoon, S., Nissen, S., Park, D., Sanford, R.A., and Löffler, F. E. (2016) Nitrous oxide reduction kinetics distinguish bacteria harboring clade I NosZ from those harboring clade II NosZ. *Appl Environ Microbiol* **82**: 3793–3800.

Zhang, H., Yohe, T., Huang, L., Entwistle, S., Wu, P., Yang, Z., *et al*. (2018) dbCAN2: a meta server for automated carbohydrate-active enzyme annotation. *Nucleic Acids Res* **46**: W95–W101.

Zhou, Z., Liu, Y., Xu, W., Pan, J., Luo, Z.-H., and Li, M. (2020) Genome- and community-level interaction insights into carbon utilization and element cycling functions of Hydrothermarchaeota in hydrothermal sediment. *mSystems* **5**: e00795-00719.

Zhu, X., Burger, M., Doane, T.A., and Horwath, W.R. (2013) Ammonia oxidation pathways and nitrifier denitrification are significant sources of N_2O and NO under low oxygen availability. *Proc Natl Acad Sci USA* **110**: 6328–6333.

Supporting Information

Additional Supporting Information may be found in the online version of this article at the publisher's web-site:

Table S1. 16S rRNA gene sequence identities from query sequences to top ten organisms hits by BLASTN.

Table S2. 16S rRNA gene sequence identities between *Ca*. Sulfidibacteriales sequences by BLASTN.

Table S3. AAI values from Bin4 to Bacteroidetes in other orders calculated by compareM.

Table S4. The list of the annotated genes of Bin4 in Fig. 4.

Table S5. Carbohydrate-active genes of Bin4 annotated on the dbCAN webserver.

Table S6. Genes encoding proteases and peptidases of Bin4 identified against the MEROPS database.

Table S7. The list of the annotated genes in Fig. 5.

Table S8. Statistical summary of the chemoautotrophic enrichment genomes.

Table S9. The identity between the isolate and Bin4 calculated by JSpeciesWS.

Table S10. The growth ability of the isolate with different electron accepters.

Table S11. Nine pairs of SusC/SusD and surrounding glycoside hydrolases (GHs) identified in the genome of Bin4.

Table S12. Geographic locations of *Ca*. Sulfidibacteriales.

Table S13. 43 conserved marker genes used to infer the genome tree.